해양과학기술논문집 제14권 제2호(2005)
Bull. Mar. Sci. & Tech., 14(2) : 133-146(2005)

BULLETIN OF
MARINE SCIENCE
AND TECHHNOLOGY

Alkenone production in the upper 200 m of the Pacific Ocean

Kyung Eun Lee[a,*], Ralph Schneider[b]

[a]*Division of Ocean Science, Korea Maritime University, Busan 606-791, South Korea*
[b]*Département de Géologie et Océanographie, Université de Bordeaux 1, 33405 Talence, France*

Received 2 September 2003; received in revised form 8 November 2004; accepted 8 November 2004
Available online 28 January 2005

Abstract

To investigate the depth of alkenone production in the Pacific Ocean, seawater samples were collected and filtered for suspended material from the surface mixed layer, as well as from the water depths of 100, 150 and 200 m during the May–June 2002 IOC cruise aboard the R/V *Melville* and September 2002 Daeyang cruise by the R/V *Onuri*. The concentrations of total C_{37} alkenones were measured and compared to those of chlorophyll a measured during the same cruise. Results show that the vertical distribution of alkenone abundance appears to be consistent with changes in chlorophyll concentration. In the western boundary current and equatorial regions, where the chlorophyll maximum occurs near the surface, the alkenone concentration maximum exists near the surface. In contrast, in the subtropical gyre, where the chlorophyll maximum occurs in the subsurface, the alkenone concentration maximum occurs at the depth of the chlorophyll maximum (~100 m). Comparison of alkenone-based temperature estimates with CTD in situ temperatures reveals that they are mostly consistent with each other. Our results suggest that in the western boundary and equatorial regions alkenones seem to be produced at or close to the sea surface, whereas in the subtropical gyre center a subsurface production could be of importance for the flux from the surface to the bottom.

Keywords: *Emiliania huxleyi*; Alkenones; Sea surface temperature; Chlorophyll maximum; Suspended particulates; Pacific

1. Introduction

Paleotemperature reconstruction by alkenones is based on the widely accepted hypothesis that some haptophyte microalgae produce long chain (C_{37}) unsaturated ketones whose degree of unsaturation changes with environmental temperature. Since Brassell et al. (1986) showed that the degree of unsaturation of C_{37} alkenones is related to variations in sea surface temperature (SST), numerous studies have been conducted to verify the applicability of this technique to paleotemperature estimates. The relationship between alkenone unsaturation index ($U^k_{37} = (C_{37:2})/((C_{37:2}) + (C_{37:3}))$) and temperature of seawater in which alkenone-producing algae grow has been

*Corresponding author. Tel.: +82 51 410 4759; fax: +82 51 404 3538.
E-mail address: kyung@bada.hhu.ac.kr (K.E. Lee).

0967-0637/$ - see front matter © 2004 Elsevier Ltd. All rights reserved.
doi:10.1016/j.dsr.2004.11.006

K.E. Lee, R. Schneider / Deep-Sea Research I 52 (2005) 443–456

calibrated using results from laboratory culture experiments with a single strain of *Emiliania huxleyi* (e.g. Prahl et al., 1988), and results of analysis of surface water and sediment trap samples (e.g. Prahl and Wakeham, 1987; Prahl et al., 1993; Conte et al., 2001), and coretop sediments (e.g. Müller et al., 1998). These studies suggest that the relationship between $U^{k'}_{37}$ values and seawater temperature is generally linear, and the relationship has been applied to numerous studies on the reconstruction of past SST measuring long chain alkenones extracted from marine sediments.

However, it is still uncertain that $U^{k'}_{37}$ temperature is truly representative of the SST. Recently published review papers on alkenone thermometer calibrations (e.g. Prahl et al., 2000; Bijma et al., 2001; Herbert, 2001) suggest that growth temperature may vary from SST. In certain areas, significant production of alkenones may occur below the surface mixed layer (e.g. Prahl et al., 1993; Ternois et al., 1997; Bentaleb et al., 1999; Ohkouchi et al., 1999). In that case, the alkenone-based temperature estimates from the marine sediments could be biased toward a subsurface temperature that is significantly colder than the surface temperature. Also various studies (e.g. Epstein et al., 2001; Prahl et al., 2003) documented that physiological factors other than growth temperature, such as nutrient and light availability, could influence the $U^{k'}_{37}$ values. In addition, in the warm surface waters of the western Pacific ocean (>26.4 °C), where the associated $U^{k'}_{37}$ is close to a value of 1.0, the unsaturation index cannot be used as an accurate paleothermometer (Bentaleb et al., 2002).

In this study, seawater samples from the top 200 m in the water column of the western Pacific were analyzed in order to evaluate the depth of alkenone production. We have analyzed the concentrations of C_{37} alkenones and compared them to the concentrations of chlorophyll and nutrients measured during the same cruise. Also the spatial and vertical distribution pattern of the alkenone concentration was compared to that of coccolithophores published by others. The estimates of alkenone-based temperatures were compared to those from CTD in situ measurements. Results from these analyses will help us to understand the effects of natural variability in the depth of alkenone biosynthesis on $U^{k'}_{37}$ -based temperature estimates from marine sediments.

2. Material and analytical methods

2.1. Sampling

Seawater samples were collected during the 2002 IOC cruise (May 1–June 6) and 2002 Daeyang cruise (August 25–September 6). The IOC cruise covers a latitudinal range from 50°N to 22°N including subarctic, transitional, and subtropical provinces of the western North Pacific, and the Daeyang cruise covers one station (station PNG) in the equatorial area (Fig. 1). The first station (station 1) was occupied in the Kuroshio off the east coast of Japan. Station 2, at the subarctic gyre western boundary, was occupied at the Japanese JGOFS time series Station (KNOT), which is the presumed formation region of the North Pacific Intermediate Waters (NPIW), and is also the region of high nutrient surface waters. Station 3 was located in the subarctic gyre of high nutrient surface waters and the formation region of the NPIW. Station 4 was in the confluence zone

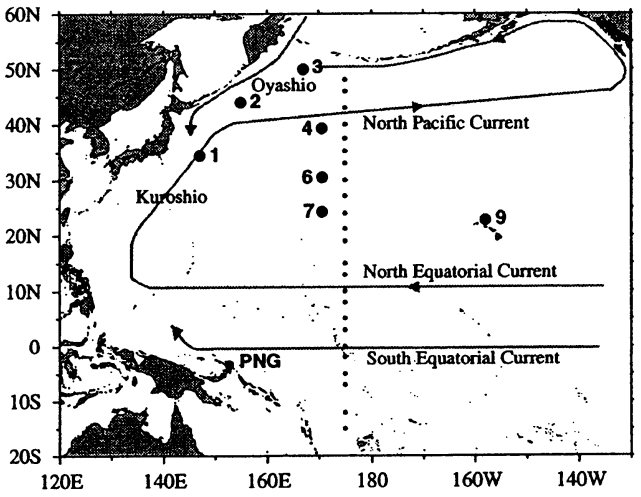

Fig. 1. Location of study area. Big dot indicates the location of stations. Small dot indicates the location of surface sediment reported by Ohkouchi et al. (1999). Arrows indicate general flow direction of the currents (Van Scoy and Druffel, 1993).

between the waters of the Oyashio and the Kuroshio. Station 6 was in the North Pacific subtropical gyre center with the low-nutrient surface waters. Station 7 was also in the North Pacific subtropical gyre. Station 9, located further east compared to the station 7, was occupied at the JGOFS/WOCE Hawaii Ocean Time-series station ALOHA, which was also in the North Pacific subtropical gyre waters. The final station PNG was located in the South Equatorial Current in the western Pacific equatorial area off New Ireland Island, Papua New Guinea.

Seawaters were collected at the depth of the surface mixed layer and at 100, 150, and 200 m in CTD bottles. Volumes filtered for analysis were 40 to 100 L for each sample (see Table 1). Combusted (500 °C for 24 h) GFF filters were used for all samples. Sample filters were immediately stored at −20 °C after the filtration until analysis. Ancillary data including seawater temperature, chlorophyll a, and nutrients were provided by other participants of the 2002 IOC cruise. Water temperatures were measured at the same time of CTD bottle sampling. Chlorophyll a contents were measured on board with seawater samples collected from the CTD bottle casts. Seawater samples for chlorophyll were from the depths of 10, 20, 30, 40, 50, 60, 70, 80, 100, 150, and 200 m. Nutrients were also measured on board with seawater samples from the CTD bottle casts and measured by Technicon Nutrient Autoanalyzer. Seawater samples for nutrients were at 10 m intervals from 10 to 100 m, at 150 m, at 100 m intervals from 200 to 1500 m, and at 500 m intervals from 2000 to 5000 m.

2.2. *Alkenone analysis*

Filter samples were analyzed at the University of Bremen. Analytical procedures have been published elsewhere (Müller and Fischer, 2001). Long-chain alkenones were extracted from filters by ultrasonication using a UP 200 H sonic disruptor probe (200W, amplitude 0.5, pulse 0.5) with successively less polar mixtures of methanol and methylene chloride (MeOH, MeOH/CH_2Cl_2 1:1, CH_2Cl_2), each for 3 min.The combined extracts were cleaned by elution with methylene chloride through a commercial silica cartridge. Saponification was then performed at 80 °C for 2 h with 0.1 M KOH in 90/10 CH_3OH/H_2O. The alkenone fraction was obtained by partitioning into hexane. The final extracts were analyzed by capillary gas chromatography with a HP 5890A, a 50 m fused silica column (0.32 mm × 0.52 mm), and flame ionization detection. The oven temperature was programmed from 50 to 150 °C at 30 °C min^{-1}, from 150 to 230 °C at 8 °C min^{-1}, and from 230 to 320 °C at 6 °C min^{-1}, and the final temperature was maintained for 45 min.

Quantification of C_{37} alkenones was achieved with squalane as internal standard and the relative response factors of the C_{38} and C_{39} n-alkanes. The measured concentrations of the C_{37} alkenones near detection limit are in the range of 0.6–1.5 ng L^{-1} in this study. $U^{K'}_{37}$ temperature estimates were based on the calibration of Prahl et al. (1988) ($U^{K'}_{37} = 0.034T + 0.039$).

3. Results

3.1. *Temperature, salinity and nutrients*

The measured vertical distributions of temperature, salinity and nutrients in the upper 200 m water column are presented in Fig. 2. The surface mixed layer is defined as the layer between the surface and a depth of 20–100 m with temperatures similar to those at the surface. At stations 1, 6, 7, and 9 in mid latitudes, the thickness of the surface mixed layer is 20–40 m. At station 2, it is 70 m thick. At station PNG in the equatorial area, it is 100 m thick. The thermocline occurs at depths below the surface mixed layer and extends to 1000 m at stations 1, 6, 7, 9 and PNG. At stations 2 and 3 in high latitudes, the main thermocline is not present. Instead, a dicothermal layer, a layer of cold water sandwiched between the warmer surface and deeper layers, occurs at 60–150 m at station 2, and 90–125 m at station 3.

The salinity of the surface waters is high at station PNG, and low at high latitudes (Fig. 2). The vertical salinity distribution shows that in the tropics, there is a sharp salinity maximum at 100–200 m depth. In the subtropical regions, the

Table 1
Analytical results of seawater samples from the Pacific

Station	Depth (m)	Water Vol.(L)	$C_{37:3}$ (ng/L)	$C_{37:2}$ (ng/L)	Total C_{37} (ng/L)	$U^{K'}_{37}$ T.[a] (°C)	$T_{in\ situ}$ (°C)	U^{K}_{38Me}	U^{K}_{38Et}	C_{37}/C_{38}	Chl.	NO_3 (μM)	SiO_2 (μM)	PO_4 (μM)
ST1	(34°N	26.1	147°E	4.9)										
	20	60	14.40	33.82	48.39	19.5	20.5	0.64	0.86	1.32	0.66	0.00	0.01	0.00
	100	100	0.78	2.15	3.09	20.4	19.1	0.70	0.86	1.45	0.07	1.62	3.55	0.10
	150	100	0.61	1.66	2.34	20.4	18.2	0.67	0.84	1.50	0.03	2.10	3.84	0.12
	200	90	0.27	0.63	1.08	19.3	17.6	—	—	—	0.01	4.16	4.54	0.18
ST2	(44°N	155°E)												
	20	100	1.83	0.30	3.35	3.0	3.6	0.08	0.28	1.86	0.38	19.02	39.12	1.57
	100	100	0.16	0.06	0.39	—	1.5	—	—	—	0.04	23.11	43.53	1.94
	150	100	0.12	0.13	0.26	—	2.4	—	—	—	0.05	37.06	79.22	2.83
	200	100	0.09	0.18	0.31	—	3.1	—	—	—	0.01	42.30	99.15	3.36
ST3	(50°N	167°E)												
	20	100	0.39	0.55	1.04	—	2.6	—	—	—	0.47	22.25	41.03	1.55
	100	100	0.07	0.00	0.16	—	1.6	—	—	—	0.15	24.48	44.70	1.75
	150	100	0.00	0.06	0.06	—	3.5	—	—	—	0.01	39.17	83.68	2.78
ST4	(39°N	19.2	170°E	33)										
	10	70	0.07	0.10	0.34	—	11.8	—	—	—	0.77	5.79	15.83	0.41
	60	80	0.07	0.09	0.20	—	9.6	—	—	—	0.06	13.44	18.37	0.88
	100	80	0.07	0.06	0.21	—	9.0	—	—	—	0.03	14.51	20.76	1.11
	150	90	0.10	0.09	0.27	—	7.9	—	—	—	0.01	15.79	22.93	1.23
	200	100	0.17	0.15	0.35	—	7.7	—	—	—	0.00	19.67	29.40	1.35
ST6	(30°N	30	170°E	35)										
	10	80	36.66	88.05	124.92	19.6	20.4	0.62	0.84	1.06	0.10	0.00	0.01	0.01
	50	80	29.18	27.90	57.14	13.2	17.2	0.42	0.68	1.15	0.25	0.05	0.05	0.08
	100	100	1.23	1.47	2.76	14.8	16.5	0.39	0.67	1.23	0.23	3.47	3.85	0.20
	200	100	0.23	0.38	0.63	17.2	15.4	0.47	0.72	1.19	0.01	7.63	7.66	0.48
ST7	(24°N	15	178°E	20)										
	20	100	0.24	1.59	1.88	24.3	24.6	0.82	0.93	1.23	0.06	0.01	0.35	0.01
	100	100	1.04	4.56	5.62	22.8	21.9	0.69	0.91	1.11	0.17	3.51	4.31	0.22
	150	100	0.20	0.46	0.70	19.2	19.4	0.45	0.82	1.89	0.12	6.43	6.17	0.28
	200	100	0.03	0.06	0.08	—	17.3	—	—	—	0.02	7.66	7.88	0.51
ST9	(22°N	45	158°W)											
	10	100	0.05	0.05	0.13	—	25.7	—	—	—	0.06	0.00	0.06	0.00
	50	40	0.05	0.59	0.68	—	23.1	—	—	—	0.09	0.16	0.34	0.00
	100	100	0.74	2.77	3.54	22.1	21.5	0.67	0.90	1.16	0.17	0.47	0.56	0.07
	150	100	0.02	0.24	0.27	—	19.6	—	—	—	0.09	2.37	1.25	0.15
	200	100	0.01	0.21	0.23	—	18.0	—	—	—	0.02	2.42	2.52	0.24
PNG	(3°S	22	152°E	47)										
	10	100	0.31	10.39	10.86	27.4	28.5	0.66	0.96	1.24	—	—	—	—
	125	100	0.18	1.27	1.45	—	24.1	—	—	—	—	—	—	—
	150	100	0.03	0.57	0.67	—	22.0	—	—	—	—	—	—	—
	200	100	0.02	0.11	0.16	—	17.2	—	—	—	—	—	—	—

[a] $U^{K'}_{37}$ T. was calculated from $U^{K'}_{37}$ value using the published calibration equation of Prahl et al. (1988).

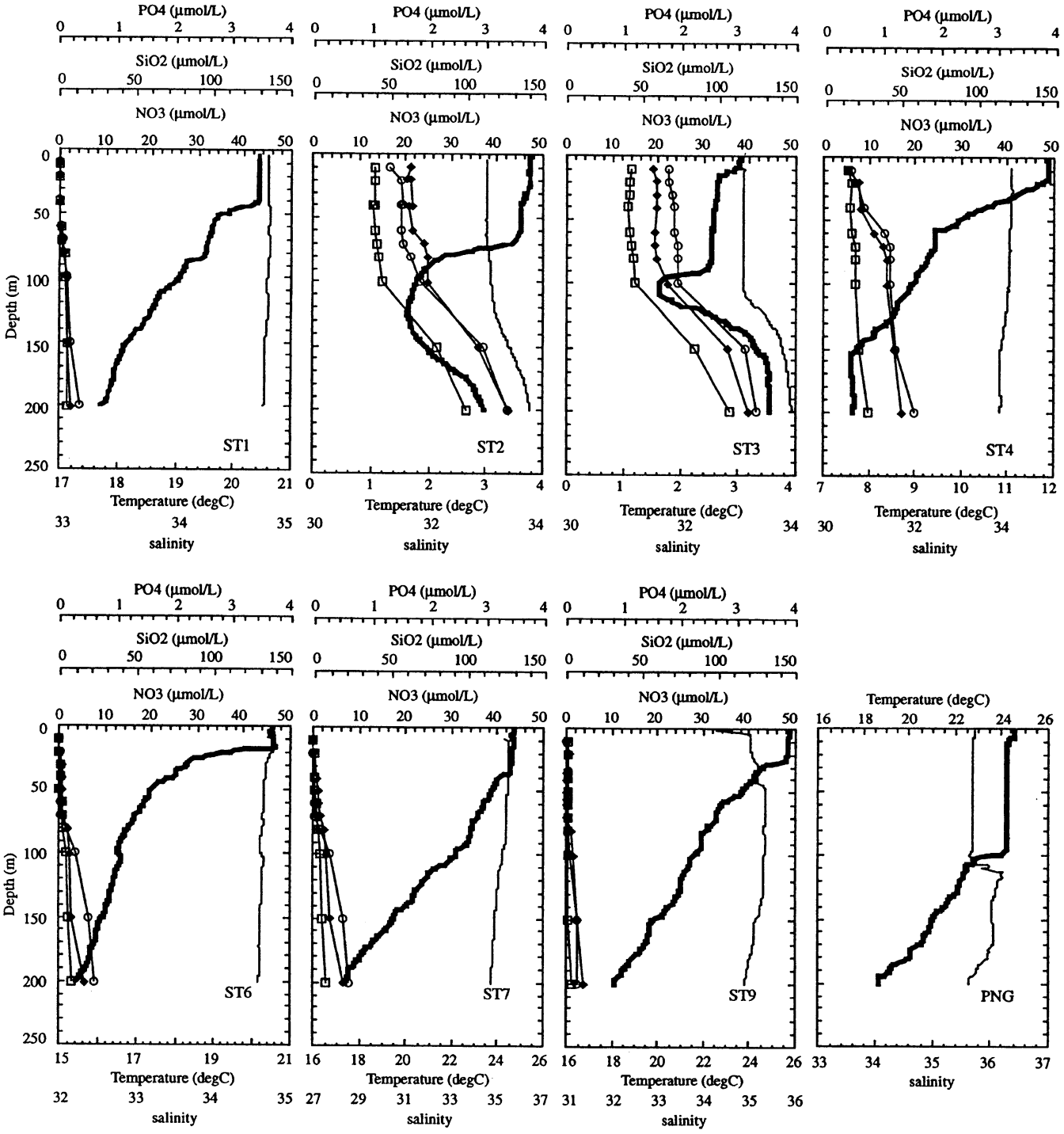

Fig. 2. The vertical profiles of temperature, salinity, and nutrients concentration (nitrate, phosphate and silicate) in the upper 200 m water column measured during the sampling cruise. Thick line indicates temperature. Thin line indicates salinity. Open circle indicates the concentration of nitrate. Open rectangle indicates the concentration of silicate. Closed diamond indicates the concentration of phosphate.

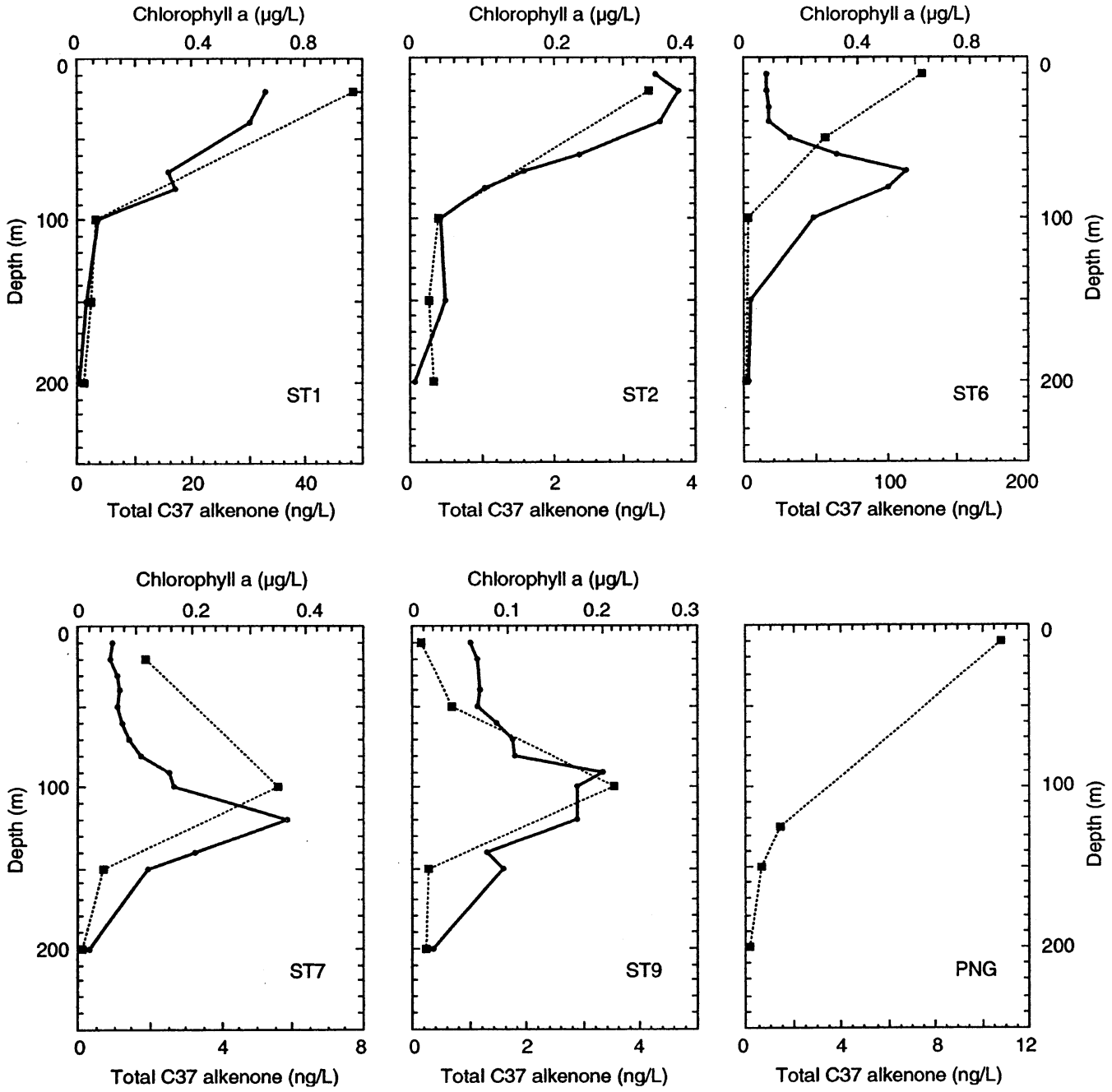

Fig. 3. The vertical distributions of total C_{37} alkenone and chlorophyll a. Straight line indicates chlorophyll data. Dash line indicates total C_{37} alkenone data.

salinity decreases slightly with depth in the upper 200 m. In high latitudes, the salinity generally increases with depth beneath 100 m depth.

Measurements of nutrient concentration during the 2002 IOC cruise (Fig. 2) show that the concentration of nitrate is in the range of 16–23 μM at the surface at stations 2 and 3 and it is 6 μM at the surface in station 4. The nitrate concentrations are extremely low (<1 μM) at the surface at stations 1, 6, 7, and 9. The distribution

patterns of phosphate and silicate at the surface are similar to that of nitrate. Beneath 100 m depth, the nutrient concentrations increase rapidly with increasing depth. In high latitudes (stations 2 and 3), the nitrate concentration increases greatly as the depth increases to 200 m, whereas in mid latitudes (stations 1, 6, 7, and 9), the concentration increases slightly as the depth increases. The vertical distribution patterns of phosphate and silicate are similar to that of nitrate.

3.2. *Alkenone and chlorophyll concentrations*

The concentrations of total C_{37} alkenones ranged over three orders of magnitude (Fig. 3 and Table 1). The alkenone concentration in the surface mixed layer is relatively low in the subarctic waters (<1–$3\,ngL^{-1}$ at stations 2 and 3), whereas it is relatively high in the Kuroshio (1–$50\,ngL^{-1}$ at station 1) and subtropical (<1–$125\,ngL^{-1}$ at stations 6, 7, and 9) and equatorial (<1–$11\,ngL^{-1}$ at station PNG) waters.

At station 1 in the Kuroshio, the concentration of total C_{37} alkenones is high in the surface mixed layer and decreases with depth. GC chromatogram indicates that samples from the surface mixed layer to the depth of 200 m contain enough long chain alkenones to be analyzed. At station 2 in the subarctic gyre, alkenone concentration is enough to be analyzed in the surface mixed layer, but too low below the depth of 100 m. At stations 3 and 4, samples from all depths contain very low amounts of alkenones. At station 6, alkenone concentration is high in the surface mixed layer, and still high at the depth of 50 m. At this station, the alkenone concentration is low at the depth of 100 and 200 m. At stations 7 and 9, the highest alkenone concentration occurs at the depth of 100 m. At station 7 the concentration in the surface mixed layer is still enough to be analyzed, but at station 9 the concentration at the surface is too low to be analyzed. At station PNG in the equatorial region, the concentration is high in the surface mixed layer, but too low to measure below the depth of 100 m.

Chlorophyll a measurements during the 2002 IOC cruise reveal that the concentration at the surface is relatively high in the subarctic waters (0.3–$0.7\,\mu gL^{-1}$ at stations 2 and 3) and low in the subtropic waters (0.05–$0.1\,\mu gL^{-1}$ at stations 6, 7, and 9) (Fig. 3). The values of chlorophyll concentration at stations 1–4 decrease rapidly below the surface mixed layer (Fig. 3). In the subtropical gyre, the chlorophyll maximum values in the subsurface are in the range of 0.2–$0.3\,\mu gL^{-1}$ (except station 6, $\sim 0.6\,\mu gL^{-1}$). Based on the vertical distribution pattern of chlorophyll a concentration, all stations can be grouped into two categories: (1) stations at which chlorophyll maximum occurs near the surface mixed layer (stations 1–4, and station PNG), and (2) stations at which the chlorophyll maximum occurs in the subsurface (stations 6, 7, and 9).

3.3. $U_{37}^{k'}$ *temperatures*

At station 1, CTD-measured temperature ranges from 20.4 °C in the surface mixed layer to 17.6 °C at the depth of 200 m (Fig. 4). The temperature estimated from the $U_{37}^{k'}$ is 19.5 °C near the surface and 19.3 °C at the depth of 200 m. It appears that all alkenone-based temperature estimates from the surface mixed layer to the 200 m depth are similar to the surface temperature indicating that the surface signal is dominant through the upper 200 m of the water column. At station 2, the alkenone-based temperature estimate is 3.0 °C, close to the measured value of 3.8 °C. Alkenone concentration below the depth of 100 m is too low to estimate the $U_{37}^{k'}$ temperature. At station 6, there are discrepancies between CTD-measured temperatures and alkenone-based temperatures. CTD-measured temperatures are 20.5, 17.3, 16.5 and 15.4 °C at 10, 50, 100, and 200 m respectively, whereas alkenone-based temperatures are 19.6, 13.2, 14.8, and 17.2 °C at each depth. Compared to station 6, alkenone-based temperature estimates at station 7 are very consistent with CTD-measured temperatures. The CTD-measured temperatures are 24.5, 22.0 and 19.4 °C at 20, 100, and 150 m respectively, whereas the alkenone-based temperatures are 25.3, 22.8 and 19.2 °C. At station 9 the only available alkenone-based temperature is from the chlorophyll maximum depth because of low concentration of alkenone at the surface and the deeper part. The alkenone-based temperature is

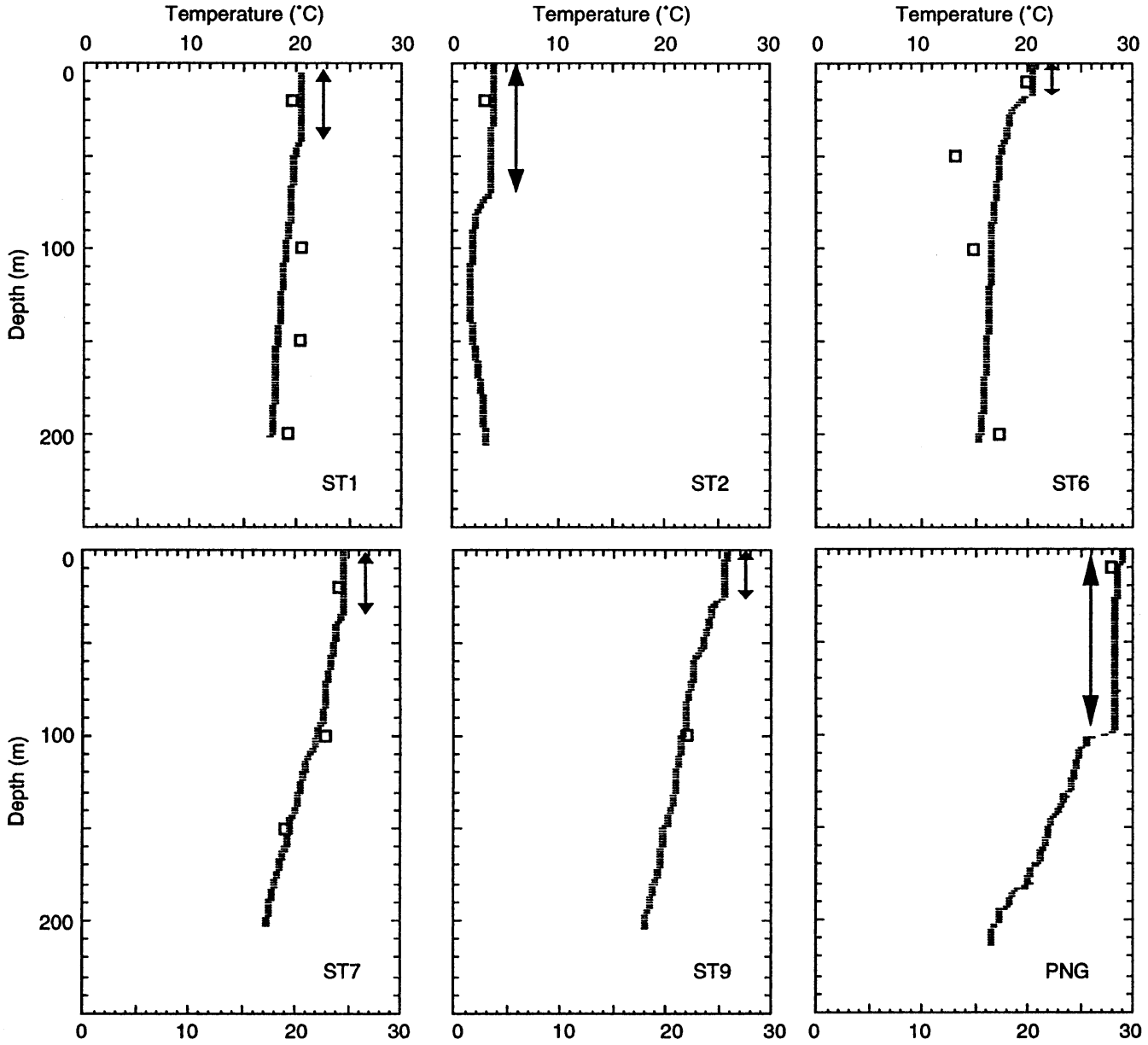

Fig. 4. The vertical distributions of CTD-measured temperature and alkenone-based temperature. Open rectangle indicates alkenone-based temperature. Closed rectangle indicates CTD-measured temperature. Arrow indicates the surface mixed layer.

22.1 °C at the depth of 100 m, which is consistent with the CTD-measured temperature of 21.4 °C. At station PNG the only available alkenone temperature is from the surface mixed layer because of low concentration of alkenone at depth. The alkenone temperature is 27.4 °C, while the CTD-measured temperature is 28.5 °C.

4. Discussion

4.1. Depth range of alkenone production

A comparison between the concentrations of total C_{37} alkenones and those of chlorophyll a measured during the same cruise shows that the vertical distribution of alkenone is consistent with

that of chlorophyll concentration. In the western boundary current area, where the chlorophyll maximum occurs near the surface, the alkenone concentration maximum exists near the surface. In contrast, in the subtropical gyre, where the chlorophyll maximum occurs at the subsurface, the alkenone concentration maximum occurs at the depth of the chlorophyll maximum (~100 m) except station 6. Since the long-chain alkenones are produced by haptophyte microalgae, it is likely that the depth of maximal production of alkenone coincides with the depth of primary production maximum and chlorophyll maximum. Our results are comparable to the results of Prahl et al. (1993). They found that during the periods of water stratification in the northeast Pacific alkenone production occur at the subsurface chlorophyll maximum rather than in the surface mixed layer. It can be expected that the lack of nutrients at the surface limits growth of phytoplankton in the subtropical waters.

Alkenone abundances were also compared to coccolithophore abundances. Okada and Honjo (1973) investigated extensively and quantitatively the distribution pattern of coccolithophores in the North Pacific. According to their study, *Emiliania huxleyi*, widely regarded as the most likely source of long chain alkenones, has a wide vertical distribution through the upper 200 m from the polar to tropical ocean. In high latitudes (50°–40°N) and low latitudes (5°N–5°S), *E. huxleyi* is present at all depths with high abundance between the surface and 100 m depth. In the subtropical area, however, the highest abundance of *E. huxleyi* occurs at the depth of 100–120 m (Reid, 1980). Recently Cortés et al. (2001) investigated coccolithophore abundances in samples from the upper 200 m of the water column at monthly intervals between January 1994 and August 1996 at the HOT station ALOHA, Hawaii. Their data show that the relatively high density of *E. huxleyi* occurs at the depth of 75–150 m with maximum centered between 100 and 150 m during 1994–1996 except in January 1995, when the highest density occurred near the surface. Okada and Honjo (1973) show that *Gephyrocapsa oceanica*, another source of alkenones (Marlowe et al., 1990; Volkman et al., 1995), dominates in the top 100 m of the water column only at low latitude. Therefore, the distribution patterns of both *E. huxleyi* and *G. oceanica* support our results that alkenone production depth is near the surface in the high latitude and the equatorial regions, and deeper in the subtropical area.

It has been reported that photosynthetic pigment data can be used to characterize the broad algal classes, although many algal classes do not have unique pigments that can allow unambiguous identification in a given sample. HPLC pigment analysis with electronic observations suggests that prymnesiophytes contain 19′-hexanoyloxyfucoxanthin as a diagnostic pigment (Andersen et al., 1996). Especially, 19′-hexanoyloxyfucoxanthin is considered to be the major carotenoid of *E. huxleyi* as well as another prymnesiophyte *Crymbellus aureus* (Wright and Jeffrey, 1987). In the North Pacific central gyre, the concentration maximum of 19′-hexanoyloxyfucoxanthin occurs at the subsurface along the 158°W transect (120 m depth at 27°N and 100 m depth at 30°N) during April 1998, and it is consistent with the vertical distribution pattern of chlorophyll a (Leonard et al., 2001). Near the Kuroshio region in the East China Sea, the concentration maximum of 19′-hexanoyloxyfucoxanthin and chlorophyll a exists in the surface mixed layer in spring (Furuya et al., 2003). The above results of 19′-hexanoyloxyfucoxanthin analysis from others are consistent with our alkenone abundance data in the North Pacific central gyre and Kuroshio region.

The alkenone abundance data in this study indicate that alkenone production depth seems to be at or near the surface mixed layer in the western boundary current and the equatorial regions, and deeper than the surface mixed layer in the subtropical gyre region. The vertical distribution pattern of alkenone concentration for station 6 is anomalously different from that of the chlorophyll concentration. The alkenone temperature estimates are also different from those of CTD-measured temperatures at the same depth. The reason is not clear. There is a possibility that the alkenones may be transferred from another area. At all stations, the alkenone concentration is extremely low at the depth of 200 m, indicating

that the alkenone production may not be significant below 200 m in the water column.

4.2. *Calibration equation*

In this study, the calibration equation of Prahl et al. (1988) was used to estimate the alkenone temperatures for all samples. Prahl et al. (1988) established the equation based on laboratory culture experiments of *E. huxleyi* collected from the northeastern Pacific. Interestingly, the equation is very similar to that derived from surface sediment analysis (Müller et al., 1998). In Fig. 5(a), the $U^{k'}_{37}$ index values are compared to CTD-measured temperatures at the sampling depth. All data points from the water column were included. The dashed line indicates the calibration equation. Data from the depths of maximum alkenone abundance at each site are highlighted with a closed circle. For this subset of data, the linear relationship between them suggests excellent correspondence between $U^{k'}_{37}$ index and CTD-measured temperature.

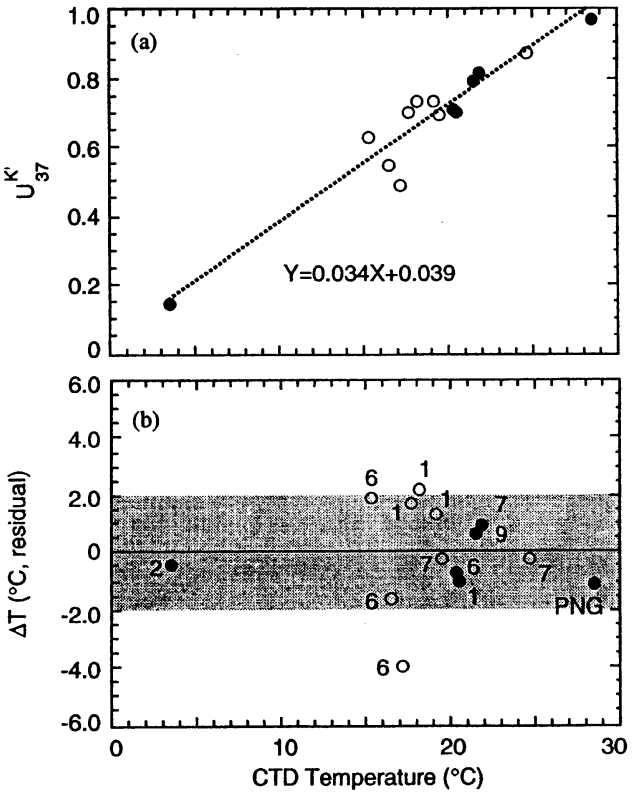

Fig. 5. (a) A comparison between the values of alkenone unsaturation index and CTD-measured temperature at the sampling depth. Especially, closed circle represents the data point from the sample depth with maximum alkenone concentration in each station. Open circle represents other data points. Dash line represents the calibration equation of Prahl et al. (1988). (b) The difference between alkenone-based temperature and CTD-measured temperature at the same depth. Closed circle represents the data point from the sample depth with maximum alkenone concentration in each station. The number indicates the station.

The various calibration studies based on culture experiments and field measurements (Volkman et al., 1980; Marlowe et al., 1984; Prahl and Wakeham, 1987; Prahl et al., 1988; Brassell, 1993; Volkman et al., 1995) show different correlations between $U^{k'}_{37}$ and ocean water temperature. Culture experiments with *G. oceanica* show that the relationships between $U^{k'}_{37}$ and temperature are different from those of *E. huxleyi* (Volkman et al., 1995). In addition, water column studies illustrate the genetic variation in the $U^{k'}_{37}$ and temperature relationship in a single species (e.g. Conte et al., 1998). However, our results show that the alkenone-based temperature estimated from the Prahl et al. calibration equation is comparable to the CTD-measured temperature at the depth of maximum alkenone abundance, suggesting that the calibration equation established from laboratory culture experiments is applicable to field measurements although the organic compounds are synthesized by genetically diverse populations under natural oceanic condition.

The deviations from the alkenone-temperature calibration line for all data points in this study are illustrated in Fig. 5 (b). The deviations (alkenone temperature minus CTD temperature) are in the range of ±2 °C. The deviations at the depth of maximum alkenone abundance are less than 1 °C. At station 1, the alkenone temperature estimates at the depth of 100, 150 and 200 m are higher than CTD-measured ones at the same depth, but they are similar to surface temperature. Note that the maximum alkenone abundance occurs in the surface mixed layer at station 1. It seems that the surface alkenone temperature signal is dominant through the upper water column at station 1. At stations 2 and PNG, another place where the maximum alkenone abundance occurs in the surface mixed layer, it is difficult to estimate

alkenone temperatures below the surface mixed layer because of the low alkenone concentration at the depth. Therefore, it is not sure that the surface alkenone temperature signal is dominant through the upper water column in the area. However, considering the low production at the subsurface in these regions, it is conceivable that the surface signal is dominant through the upper water column in the area where the maximum alkenone production occurs at the surface.

Previous studies on the alkenone calibration equation compared the alkenone temperatures to the sea surface temperatures. In Fig. 5 in this study, however, alkenone temperatures from the water column were compared to CTD temperatures at the sampling depth with the assumption that the alkenones are produced at the depth. (Data from station 6 may not be the case.) A comparison of alkenone temperature with the sea surface temperature (Fig. 6) shows that the deviations (SST minus alkenone temperature) are in the range of 0.1–7.2 °C. All values are positive, which means that all alkenone-based temperature estimates are colder than the sea surface temperatures. Especially at stations 7 and 9, where the maximum alkenone abundance occurs at the subsurface, the differences between sea surface temperature and alkenone temperature are 1.8 and 3.6 °C. Situations like this could cause error in the

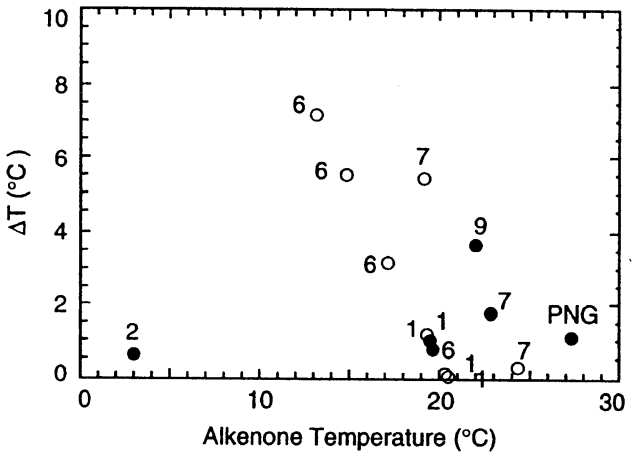

Fig. 6. The difference between sea surface temperature and alkenone-based temperature. Closed circle represents the data point from the sample depth with maximum alkenone concentration in each station. The number indicates the station.

reconstruction of paleotemperature from marine sediments.

Physiological impacts on alkenone unsaturation index are controversial. Physiological factors such as nutrient and light stress could contribute to variability in the alkenone unsaturation index. Popp et al. (1998) show that nutrient limited growth rate effects do not produce significant error in $U^{K'}_{37}$ based paleotemperature estimates. However, Epstein et al. (1998) show that $U^{K'}_{37}$ values vary with nutrient availability and cell division rate, suggesting that alkenone-based paleotemperature estimates could be influenced by variations in nutrient concentrations as well as seawater temperatures. Recently published data by Prahl et al. (2003) also supports this, although their results on the response of $U^{K'}_{37}$ values to nutrient stress are opposite in direction to what Epstein et al. (1998) documented. According to Epstein et al. (1998), a decrease of nutrient content from 40 μM NO_x to less than 1 μM results in an increase of 0.10–0.19 in $U^{K'}_{37}$ unit (1.8–4.4 °C). However, Prahl et al. (2003) show that a decrease of nitrate (and phosphate) concentration from 75 μM (3.2 μM) to less than 1 μM (close to 0 μM) corresponds to a decrease of 0.11 in $U^{K'}_{37}$ unit (2.1 °C). Also the effects of light limitation on $U^{K'}_{37}$ values have been discussed previously (Epstein et al., 2001; Prahl et al., 2003). Epstein et al (2001) reported that alkenone unsaturation ratios changed slightly in dark experiments (an increase of 0.046 in $U^{K'}_{37}$ unit, 0.2 °C), whereas Prahl et al. (2003) show that dark experiments resulted in an increase of 0.11 in $U^{K'}_{37}$ unit (2.1 °C) for the same *E. huxleyi* strain (strain NEPCC 55a) used by Epstein et al. (2001). From the above, physiological impacts on $U^{K'}_{37}$ value are uncertain. According to our study, at stations 1, 2, 6 and 7, the estimated alkenone temperatures in the surface mixed layer are consistent with the observed CTD values. In general, light supply may not be limited at the surface during the daytime. But the nitrate concentration is near zero in the surface mixed layer at stations 1, 6, and 7, and ~19 μM at station 2. A consistency between alkenone temperature and CTD temperature of the surface waters in this study, however, indicates that the seawater temperature is a major control factor for $U^{K'}_{37}$, and the effects of nutrient

limitation on in $U^{k'}_{37}$ value may not be significant in the surface ocean in the study area. In the subsurface (100 m) where light is significantly limited, the alkenone temperatures are consistent with CTD values (e.g. stations 7 and 9), suggesting that seawater temperature is a major control factor and that darkness could not contribute to an increase of alkenone temperature. In these regions, the difference of nutrient concentration between the surface and 100 m depth is 0.5–3.5 μM for nitrate, 0.6–4.3 μM for silicate, and 0.1–0.2 μM for phosphate. Considering the difference of nutrient concentrations between the surface and the depths in the study area, it is likely that the effects of nutrient limitation on in $U^{k'}_{37}$ value should be minimal.

Unsaturation ratios of the C_{38} methyl and ethyl alkenones (U^{K}_{38Me} = 38:2Me/(38:2Me + 38:3Me), U^{K}_{38Et} = 38:2Et/(38:2Et + 38:3Et)) were also compared to CTD-measured temperatures of the seawater at the sampling depth (Fig. 7(a)). They were correlated with seawater temperatures. However, there were consistent offsets between them. In study area, U^{K}_{38Me} values are consistently lower than $U^{k'}_{37}$, whereas U^{K}_{38Et} values were consistently higher than $U^{k'}_{37}$. In Fig. 7(b), U^{K}_{38Me} and U^{K}_{38Et} values are plotted against $U^{k'}_{37}$. The unsaturation ratios of C_{37} and C_{38} alkenones appear to be correlated. From the dataset in this study, it seems that cellular regulation of alkenone unsaturation for C_{38} as well as C_{37} is controlled by temperature, although there could still be non-temperature-related influences on alkenone unsaturation. In Fig. 7(c), ratios of C_{37} alkenones to C_{38} alkenones (C_{37}/C_{38}) are plotted versus seawater temperatures. The values are in the range of 1.1–1.5, with one exception of 1.8 from the surface water of station 2. The C_{37}/C_{38} ratios are nearly identical to those observed in the *E. huxleyi* strain of the NE Pacific samples (1.0–1.5) (Conte et al., 1998), and much lower than those of the *E. huxleyi* strain in the Sargasso Sea samples (2.0–2.5) (Conte et al., 1998).

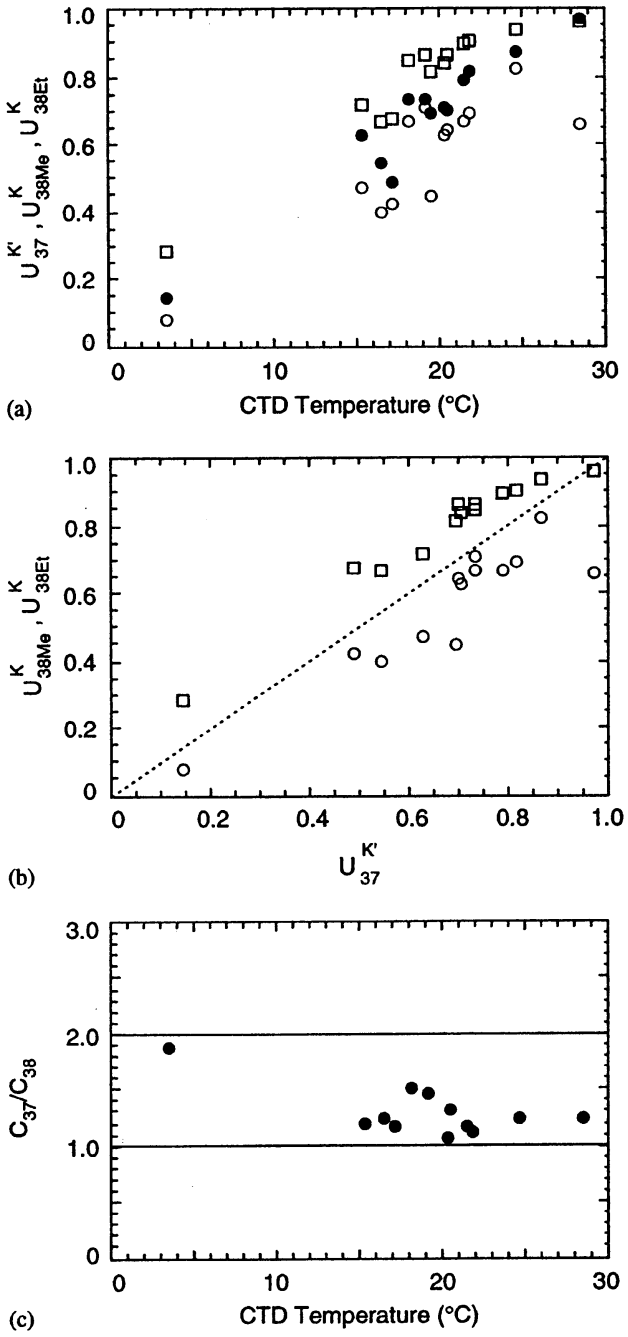

Fig. 7. (a) Unsaturation ratios of C_{37} and C_{38} alkenones versus CTD-measured temperatures. Closed circle indicates $U^{k'}_{37}$. Open circle indicates U^{K}_{38Me}. Open rectangle indicates U^{K}_{38Et}. (b) Covariance of $U^{k'}_{37}$ with U^{K}_{38Me} and U^{K}_{38Et}. Symbols are as in (a). (c) Ratios of C_{37} alkenones to C_{38} alkenones (C_{37}/C_{38}) versus CTD-measured temperatures.

4.3. Spatial distribution of alkenone production

The vertical distribution pattern of alkenone abundance is consistent with that of chlorophyll concentration in the study area. However, the spatial distribution pattern of alkenone abundance is not consistent with that of chlorophyll

concentration. The chlorophyll concentrations are relatively high in the subarctic waters, and low in the subtropic. But, the alkenone concentrations are low in the subarctic, and relatively high in the subtropic. In the Kuroshio, both chlorophyll and alkenone concentrations are high. The relatively high concentration of alkenones seems to occur in the region where the concentration of dissolved silicate is relatively low. In this region, the coccolithophorid phytoplankton community appears to be dominated over a silica-based diatom one (Brown and Yoder, 1994). It has been reported that diatoms compete well in high-nutrient (especially high silicate concentration) and cold water systems, whereas coccolithophores compete well in low-nutrient and warm water environments (Werne et al., 2000). The North Pacific subarctic waters are cold and contain high concentration of silicate, whereas the subtropical waters are relatively warm and have silica concentration of almost zero. Measurements of nutrient concentration during the 2002 IOC cruise show that the concentration of silicate is in the range of 38–42 μM in the surface water at stations 2 and 3. The silicate concentrations are extremely low (< 1 μM) in the surface water at stations 1, 6, 7 and 9. Therefore, alkenone concentration seems to be relatively high in the subtropic region although chlorophyll concentration is low in this region.

5. Concluding remarks

According to our study, in the western boundary current and the equatorial regions, detectable amounts of alkenones occur only in the surface mixed layer and alkenones produced at the subsurface are negligible. Therefore, it is conceivable that the alkenone signal from the surface mixed layer may be important to the sediment signal in these regions. In contrast, in the subtropical gyre region, alkenone abundances are greater by as much as 3–30 times in the subsurface (the depth of 100 m) than the surface mixed layer, suggesting that the subsurface production of alkenones may be significant to the sediment signal. However, further research is necessary to refine the understanding of alkenone biosynthesis, and physical and environmental controls on organic matter export from the euphotic zone to sediments.

Acknowledgments

We thank the participants in the 2002 IOC cruise by the R/V *Melville* and the 2002 Daeyang cruise by the R/V *Onuri* for their help with sampling, especially C. Measures, T. Ui, and D.S. Hahm for water sampling, K. Selph for discussions and help with chlorophyll data, G. Cutter for discussions and help with nutrient data, D. Grotheer, R. Kreutz, C. Rühlemann, and J.-H. Kim for discussions and help with alkenone analysis, and P. Müller, and F.G. Prahl for their comments and suggestions.

References

Andersen, R.A., Bidigare, R.R., Keller, M.D., Latasa, M., 1996. A comparison of HPLC pigment signatures and electronic observations for oligotropic waters of the North Atlantic and Pacific Oceans. Deep-Sea Research II 43, 517–537.

Bentaleb, I., Grimalt, J.Q., Vidussi, F., Marty, J.-C., Martin, V., Denis, M., Hatté, C., Fontugne, M., 1999. The C_{37} alkenone record of seawater temperature during seasonal thermocline stratification. Marine Chemistry 64, 301–313.

Bentaleb, I., Fontugne, M., Beaufort, L., 2002. Long-chain alkenones and $U^{k'}_{37}$ variability along a south-north transect in the Western Pacific Ocean. Global and Planetary Change 34, 173–183.

Bijma, J., Altabet, M., Conte, M., Kinkel, H., Versteegh, G.J.M., Volkman, J.K, Wakeham, S.G., Weaver, P.P., 2001. Primary signal: ecological and environmental factors-report from working group 2. Geochemistry Geophysics Geosystems 2, 2000GC000051.

Brassell, S.C., 1993. Applications of biomarkers for delineating marine paleoclimatic fluctuations during the Pleistocene. In: Engel, M.H., Macko, S.A. (Eds.), Organic Geochemistry. Plenum, New York, pp. 699–738.

Brassell, S.C., Eglinton, G., Marlowe, I.T., Pflauman, U., Sarnthein, M., 1986. Molecular stratigraphy: a new tool for climatic assessment. Nature 320, 129–133.

Brown, C.W., Yoder, J.A., 1994. Coccolithophorid bloom in the global ocean. Journal of Geophysical Research 99, 7467–7482.

Conte, M.H., Thompson, A., Lesley, D., Harris, R.P., 1998. Genetic and physiological influences on the alkenone/alkenoate versus growth temperature relationship in

Emiliania huxleyi and *Gephyrocapsa oceanica*. Geochimica et Cosmochimica Acta 62, 51–68.

Conte, M.H., Weber, J.C., King, L.L., Wakeham, S.G., 2001. The alkenone temperature signal in western North Atlantic surface waters. Geochimica et Cosmochimica Acta 65, 4275–4287.

Cortés, M.Y., Bollmann, J., Thierstein, H.R., 2001. Coccolithophore ecology at the HOT station ALOHA, Hawaii. Deep-Sea Research II 48, 1957–1981.

Epstein, B.L., D'Hondt, S., Hargraves, P.E., 2001. The possible metabolic role of C37 alkenones in *Emiliania huxleyi*. Organic Geochemistry 32, 867–875.

Epstein, B.L., D'Hondt, S., Quinn, J.G., Zhang, J., Hargraves, P.E., 1998. An effect of dissolved nutrient concentrations on alkenone-based temperature estimates. Paleoceanography 13, 122–126.

Furuya, K., Hayashi, M., Yabushita, Y., Ishikawa, A., 2003. Phytoplankton dynamics in the East China Sea in spring and summer as revealed by HPLC-derived pigment signatures. Deep-Sea Research II 50, 367–387.

Herbert, T.D., 2001. Review of alkenone calibrations (culture, water column, and sediments). Geochemistry Geophysics Geosystems 2, 2000GC000055.

Leonard, C.L., Bidigare, R.R., Seki, M.P., Polovina, J.J., 2001. Interannual mesoscale physical and biological variability in the North Pacific Central Gyre. Progress in Oceanography 49, 227–244.

Marlowe, I.T., Brassell, S.C., Eglinton, G., Green, J.C., 1984. Long chain unsaturated ketones and esters in living algae and marine sediments. Organic Geochemistry 6, 135–141.

Marlowe, I.T., Brassell, S.C., Eglinton, G., Green, J.C., 1990. Long-chain alkenones and alkyl alkenoates and the fossil coccolith record of marine sediments. Chemical Geology 88, 349–375.

Müller, P.J., Fischer, G., 2001. A 4-year sediment trap record of alkenones from the filamentous upwelling region off Cape Blanc, NW Africa and a comparison with distributions in underlying sediments. Deep-Sea Research I 48, 1877–1903.

Müller, P.J., Kirst, G., Ruhland, G., Storch, I., Rosell-Melé, A., 1998. Calibration of the alkenone paleotemperature index $U^{K'}_{37}$ based on core-tops from the eastern South Atlantic and the global ocean (60°N–60°S). Geochimica et Cosmochimica Acta 62, 1757–1772.

Ohkouchi, N., Kawamura, K., Kawahata, H., Okada, H., 1999. Depth ranges of alkenone production in the central Pacific Ocean. Global Biogeochemical Cycles 13, 695–704.

Okada, H., Honjo, S., 1973. The distribution of oceanic coccolithophorids in the Pacific. Deep-Sea Research 20, 355–374.

Popp, B.N., Kenig, F., Wakeham, S.G., Laws, E.A., Bidigare, R.R., 1998. Does growth rate affect keton unsaturation and intracellular carbon isotopic variability in *Emiliania huxleyi*? Paleoceanography 13, 35–41.

Prahl, F.G., Wakeham, S.G., 1987. Calibration of unsaturated patterns in long-chain ketone compositions for paleotemperature assessment. Nature 330, 367–369.

Prahl, F.G., Muehlhausen, L.A., Zahnle, D.L., 1988. Further evaluation of long-chain alkenones as indicators of paleoceanographic conditions. Geochimica et Cosmochimica Acta 52, 2303–2310.

Prahl, F.G., Collier, R.B., Dymond, J., Lyle, M., Sparrow, M.A., 1993. A biomarker perspective on prymnesiophyte productivity in the northeast Pacific Ocean. Deep-sea Research I 40, 2061–2076.

Prahl, F., Herbert, T., Brassell, S.C., Ohkouchi, N., Pagani, M., Repeta, D., Rosell-Mele, A., Sikes, E., 2000. Status of alkenone paleothermometer calibration: Report from working group 3. Geochemistry Geophysics Geosystems 1, 2000GC000058

Prahl, F.G., Wolfe, G.V., Sparrow, M.A., 2003. Physiological impacts on alkenone paleothermometry, Paleoceanography 18, 2002PA000803

Reid, F.M.H., 1980. Coccolithophorids of the North Pacific Central Gyre with notes on their vertical and seasonal distribution. Micropaleontology 26, 151–176.

Ternois, Y., Sicre, M.-A., Boireau, A., Conte, M.H., Eglinton, G., 1997. Evaluation of long-chain alkenones as paleotemperature indicators in the Mediterranean Sea. Deep Sea Research I 44, 271–286.

Van Scoy, K.A., Druffel, E.R.M., 1993. Ventilation and transport of thermocline and intermediate waters in the Northeastern Pacific during recent El Ninos. Journal of Geophysical Research 98, 18,083–18,088.

Volkman, J.K., Eglington, G., Corner, E.D.S., Sargent, J.R., 1980. Novel unsaturated straight chain C37–C39 methyl and ethyl ketones in marine sediments and a coccolithophore Emiliania huxleyi. In: Douglas, A.G., Maxwell J.R. (Eds.), Advances in Organic Geochemistry 1979. Oxford, UK, pp. 219–227.

Volkman, J.K., Barrett, S.M., Blankburn, S.I., Sikes, E.L., 1995. Alkeonoes in Gephyrocapsa oceanica: Implications for studies of paleoclimate. Geochimica et Cosmochimica Acta 59, 513–520.

Werne, J.P., Hollander, D.J., Lyons, T.W., Peterson, L.C., 2000. Climate-induced variations in productivity and planktonic ecosystem structure from the Younger Dryas to Holocene in the Cariaco Basin, Venezuela. Paleoceanography 15, 19–29.

Wright, S.W., Jeffrey, S.W., 1987. Fucoxanthin pigment markers of maine phytoplankton analyzed by HPLC and HPTLC. Marine Ecology Progress Series 38, 259–266.

Source : Deep-Sea Research I, (2005), 52: 443-456